Front. Mech. Eng. 2021, 16(1): 61–79
https://doi.org/10.1007/s11465-020-0611-5

RESEARCH ARTICLE

Genshen LIU, Huaiju LIU, Caichao ZHU, Tianyu MAO, Gang HU

Design optimization of a wind turbine gear transmission based on fatigue reliability sensitivity

Abstract Fatigue failure of gear transmission is one of the key factors that restrict the performance and service life of wind turbines. One of the major concerns in gear transmission under random loading conditions is the disregard of dynamic fatigue reliability in conventional design methods. Various issues, such as overweight structure or insufficient fatigue reliability, require continuous improvements in the reliability-based design optimization (RBDO) methodology. In this work, a novel gear transmission optimization model based on dynamic fatigue reliability sensitivity is developed to predict the optimal structural parameters of a wind turbine gear transmission. In the model, the dynamic fatigue reliability of the gear transmission is evaluated based on stress–strength interference theory. Design variables are determined based on the reliability sensitivity and correlation coefficient of the initial design parameters. The optimal structural parameters with the minimum volume are identified using the genetic algorithm in consideration of the dynamic fatigue reliability constraints. Comparison of the initial and optimized structures shows that the volume decreases by 3.58% while ensuring fatigue reliability. This work provides new insights into the RBDO of transmission systems from the perspective of reliability sensitivity.

Keywords gear transmission, fatigue reliability, reliability sensitivity, parameter optimization

Received May 21, 2020; accepted September 14, 2020

Genshen LIU, Huaiju LIU (✉), Caichao ZHU, Tianyu MAO
State Key Laboratory of Mechanical Transmissions, Chongqing University, Chongqing 400044, China
E-mail: huaijuliu@cqu.edu.cn

Gang HU
School of Mechatronic Engineering, Southwest Petroleum University, Chengdu 610500, China

1 Introduction

As a fundamental component of mechanical machines, gears are widely used in motion and power transmission in wind turbines, aviation, automobiles, ships, machine tools, mining, and other fields. With the growing demand for good performance under heavy-loading and high-speed-loading conditions, the fatigue reliability of gear transmission has become a crucial factor in determining the performance and service life of machines [1–5]. As an essential element of wind turbines, gear transmission is subjected to random loading conditions and numerous fatigue cycles [6,7]. The fatigue resistance of gears, including contact and bending fatigue strength, could decrease gradually due to repeated loading cycles [8]. Dynamic fatigue reliability can be explained as the capability or probability that the fatigue resistance of the gear is larger than the fatigue damage during operation. However, the common design methodology for wind turbine gear transmission usually provides the structural parameters once the basic requirements on transmission ratio, mechanical power, input speed, safety factor, and initial reliability are given [7]. From an engineering point of view, several uncertain factors, such as material properties, geometry size, and load variations, influence fatigue reliability considerably [9]. Many recent investigations have focused on the effect of uncertainties on reliability. Zhu et al. [10] quantified the effects of uncertainties, such as experiment data, material properties, and loading conditions, on the reliability of turbine bladed disks fatigue by using an experimental–numerical combined approach. Lu et al. [11] proposed the weighted regression-based extremum response surface method by considering the randomness of design parameters and the fuzziness of the safety criterion to improve structural dynamic fuzzy reliability analysis. The dynamic fatigue reliabilities of gear transmission reliability are sensitive to changes in loading conditions, material properties, design parameters, and other factors during service. Sensitivity analysis is one of effective approaches to quantify the

influence of design variables on fatigue reliability and provide rational means of fatigue design [12]. Many conditions, including complex loading conditions, dynamic fatigue reliability, and reliability sensitivity, are considered in reliability-based design optimization (RBDO) studies on gear transmissions [6,13].

Many investigations have focused on the dynamic fatigue reliability of gear transmission. These investigations considered time-variant reliability and parameter uncertainty, including dynamic fatigue reliability, random loading conditions, and transmission errors. Reliability studies can be broadly divided into three groups. The first group applies stress–strength interference (SSI) theory to evaluate the fatigue reliability of gear transmission. For example, Zhou et al. [14] developed a fatigue reliability model for the planetary gear system in a mining machine on the basis of SSI theory and in consideration of reliability sensitivity. Xie et al. [15] developed an SSI-based fatigue reliability model for a general gear system to improve reliability analysis. Random loading conditions or other factors are assumed to follow special distribution types in this group. When modeling idealization is considered, this group is generally suitable for a large range of industrial applications. The second group is based on the fatigue cumulative hypothesis for assessing fatigue reliability directly. Wang et al. [16] developed a dynamic reliability model for a 1.5 MW wind turbine gear transmission system on the basis of the fatigue cumulative hypothesis to evaluate dynamic fatigue reliability in consideration of several uncertain parameters, such as transmission error and mass density. Tan and Xie [17] proposed the concept of deterministic damage random threshold based on the median damage and probability stress–number of cycles (P-S–N) curve to solve the calculation cost issue of reliability evaluation in the application of a tractor transmission. Yan [18] used the fatigue cumulative hypothesis as a reference and developed an experimental–numerical combined approach for a 5 MW wind turbine transmission to estimate dynamic fatigue reliability. However, given that the experimental data, such as the loading distribution and P-S–N curve, of these gears is insufficient, the methods in the second group cannot be verified accurately. The third group uses the stochastic finite element method to evaluate fatigue reliability, thus providing a new methodology for fatigue design. Han et al. [19] developed such a model for a wind gear transmission by using stochastic finite element method and machine learning and considering the stochastic nature of environmental loading and internal excitations. However, this method is time consuming, especially for large-scale gear transmission systems where millions of mesh grids are generated. In summary, these studies have provided essential reliability evaluation methods for gear transmission but failed to provide feedback in terms of the reliability results and structure or parameter optimization.

Optimization design is an effective method to reduce the design flaws resulting from the incomprehensive consideration in conventional design methods. Many gear transmission optimization studies considered multiple objectives, such as structure volume, geometry parameters, and technology parameters [20–22]. Yi et al. [5] proposed a finite element and experimental modal analysis method to derive the modal properties of a 1.5 MW wind turbine gearbox. This study provided insights into structure design optimization.

The interest in RBDO studies on gear transmission is increasing nowadays. Zhu et al. [23] proposed an optimization concept based on fuzzy fatigue reliability to obtain the structural parameters for achieving the minimum volume for a large ship gear transmission in consideration of fuzzy uncertainties, such as randomness and boundary fuzziness. Qin et al. [24] considered external excitation under random loading conditions and obtained the optimal structural parameters of a 1.5 MW wind turbine gear transmission system with small volume and high reliability. Zhang et al. [25] applied the kriging agency model and the genetic algorithm to derive the compact structural parameters of a large ball mill gear transmission while ensuring fatigue reliability. Wang and Wang [26] developed a modification-based optimization model that considers the effect of the gear modification coefficient on reliability to obtain gear transmission structural parameters with low noise and sufficient reliability. Tong and Tian [27] attempted to derive the compact structural parameters of a general gearbox by applying a sensitivity-based optimization model. In summary, these investigations have provided sufficient RBDO models of gear transmissions. However, they did not consider one aspect, that is, how to bring dynamic fatigue reliability into the optimization of structural parameters.

Notably, RBDO studies on gear transmission that considered dynamic reliability sensitivity are lacking. Determination of design variables without a reliability sensitivity analysis could lead to inaccurate optimization. Several existing optimization methods for megawatt-level transmission systems disregard the quantitative analysis in the optimization of design variables and constraints [6,24,25]. A wind turbine gear transmission optimization model based on dynamic fatigue reliability sensitivity is proposed to address this issue. The dynamic fatigue reliability of the gear transmission is evaluated based on SSI theory in consideration of random loading conditions and the effect of tooth meshing characteristics. The design variables are determined based on the reliability sensitivity and correlation coefficient of the initial design parameters. By considering dynamic fatigue reliability constraints, the structural parameters for achieving the minimum volume are derived by utilizing the genetic algorithm.

2 Model description

Fatigue reliability issues associated with wind turbine gear transmission are yet to be resolved [13,28]. Investigation of the fatigue reliability of a wind turbine gear transmission is primarily related to uncertainties, such as random loading conditions and deterioration of gear fatigue strength. First, tooth contact and bending stress are calculated based on the structural parameters, load conditions, and ISO 6336 standards of gear load capacity calculation. Gear tooth time-variant meshing characteristic analysis is performed to determine the stress distributions of the teeth and gears. Residual strength theory is utilized for the evaluation of gear fatigue strength deterioration. Then, a reliability evaluation method based on SSI theory is proposed to estimate the dynamic fatigue reliability of the gear transmission. The key information from the massive initial design parameters needs to be refined for the determination of design variables and establishment of constraints in the optimization process. This issue is addressed using the reliability sensitivity and correlation coefficient of the initial design parameters. Then, the optimal structural parameters are achieved with the genetic algorithm. Figure 1 illustrates the technical flow chart of this work.

2.1 Loading conditions and structural parameters

The gear transmission structure in this study is selected from a 2 MW wind turbine gearbox, which includes the planetary stage (Stage I), intermediate parallel stage (Stage II), and high-speed parallel stage (Stage III). The three gear stages provide a total transmission ratio of 115.2 and help convert wind speed to the required speed for the generator. As displayed in Fig. 2 [29,30], Stage I is composed of the helical sun gear (s^{I}), planetary gears (p_i^{I}, $i=1$, 2, 3), and the ring gear (r^{I}). Stages II and III are composed of parallel helical gears (g_1^{II}, g_2^{II}, g_1^{III}, g_2^{III}). The load is inputted into the planetary gears (p_i^{I}), and the output is the high-speed pinion (g_2^{III}). The ring gear material studied in this work is 42CrMo, and the other gears are 18CrNiMo7–6. Ring gear manufacturing includes grinding and nitriding, and other gears involve carburizing, quenching, tempering, and grinding. Table 1 lists the main structural parameters of the transmission. Figures 3(a) and 3(b) respectively show the input torque and speed history of Stage I, which covers typical loading conditions, such as design maximum (1350.00 kN·m), mean (870.64 kN·m), and minimum (44.62 kN·m) loads, within a test time of 600 s [31,32].

2.2 Dynamic fatigue reliability evaluation

The dynamic fatigue reliability of gear transmission, which constantly changes due to random loading conditions and fatigue strength degradation, is different from the traditional design reliability determined by the safety factor. The main procedures of dynamic fatigue reliability evaluation include stress statistic calculation, fatigue strength degradation estimation, and reliability index calculation. The corresponding theories and methods, which include stress statistic calculation [17,33] and fatigue strength degradation estimation [34–37], have been discussed in several studies. The calculation of tooth stress is based on ISO 6336 standards [38,39]. Tooth bending and contact stress are calculated using the following equations.

$$\sigma_{\mathrm{F}}=\frac{F_{\mathrm{t}}}{bm_{\mathrm{n}}}Y_{\mathrm{Fa}}Y_{\mathrm{Sa}}Y_{\varepsilon}Y_{\beta}K_{\mathrm{A}}K_{\mathrm{V}}K_{\mathrm{F}\beta}K_{\mathrm{F}\alpha}, \tag{1}$$

$$\sigma_{\mathrm{H}}=Z_{\mathrm{H}}Z_{\mathrm{E}}Z_{\varepsilon}Z_{\beta}\sqrt{\frac{F_{\mathrm{t}}}{d_1 b}\frac{u+1}{u}K_{\mathrm{A}}K_{\mathrm{V}}K_{\mathrm{H}\beta}K_{\mathrm{H}\alpha}}, \tag{2}$$

where σ_{F} is the bending stress of a tooth root with the unit of $\mathrm{N\cdot mm^{-2}}$, F_{t} is the nominal tangential load with the unit of N, b is the tooth face width with the unit of mm, m_{n} is the gear module with the unit of mm, Y_{Fa}, Y_{Sa}, Y_{ε}, and Y_{β} are factors of the bending stress calculation, K_{A} and K_{V} are factors of the working condition, $K_{\mathrm{F}\beta}$ and $K_{\mathrm{F}\alpha}$ are loading distribution factors of bending stress, σ_{H} is the contact stress with the unit of $\mathrm{N\cdot mm^{-2}}$, Z_{H}, Z_{E}, Z_{ε}, and Z_{β} are factors of the contact stress calculation, d_1 is the diameter of the reference circle with the unit of mm, u is the transmission ratio, and $K_{\mathrm{H}\beta}$ and $K_{\mathrm{H}\alpha}$ are loading distribution factors of the contact stress.

Initial design parameter set $\overline{\boldsymbol{X}}$ consists of basic factor set $\overline{\boldsymbol{X}}_1$, stress calculation factor set $\overline{\boldsymbol{X}}_2$, and fatigue strength calculation factor set $\overline{\boldsymbol{X}}_3$. They can be expressed as follows:

$$\overline{\boldsymbol{X}}_1=[\beta, m_{\mathrm{n}}, Z, b, F_{\mathrm{t}}], \tag{3}$$

$$\overline{\boldsymbol{X}}_2=[Y_{\mathrm{Fa}},\ Y_{\mathrm{Sa}},\ Y_{\varepsilon},\ Y_{\beta},\ K_{\mathrm{A}},\ K_{\mathrm{V}},\ K_{\mathrm{F}\beta},\ K_{\mathrm{F}\alpha},\ Z_{\mathrm{H}},\ Z_{\mathrm{E}},\ Z_{\varepsilon},\ Z_{\beta},\ K_{\mathrm{H}\beta},\ K_{\mathrm{H}\alpha}], \tag{4}$$

$$\overline{\boldsymbol{X}}_3=[\sigma_{\mathrm{Flim}},\ Y_{\mathrm{ST}},\ Y_{\mathrm{NT}},\ Y_{\mathrm{X}},\ \sigma_{\mathrm{Hlim}},\ Z_{\mathrm{NT}},\ Z_{\mathrm{L}},\ Z_{\mathrm{v}},\ Z_{\mathrm{R}},\ Z_{\mathrm{W}},\ Z_{\mathrm{X}}], \tag{5}$$

$$\overline{\boldsymbol{X}}=\left[\overline{\boldsymbol{X}}_1,\ \overline{\boldsymbol{X}}_2,\ \overline{\boldsymbol{X}}_3\right]^{\mathrm{T}}, \tag{6}$$

where β, m_{n}, Z, b, and F_{t} are basic factors in $\overline{\boldsymbol{X}}_1$, Y_{Fa}, Y_{Sa}, Y_{ε}, Y_{β}, K_{A}, K_{V}, $K_{\mathrm{F}\beta}$, $K_{\mathrm{F}\alpha}$, Z_{H}, Z_{E}, Z_{ε}, Z_{β}, $K_{\mathrm{H}\beta}$, and $K_{\mathrm{H}\alpha}$ are stress calculation factors in $\overline{\boldsymbol{X}}_2$, and σ_{Flim}, Y_{ST}, Y_{NT}, Y_{X}, σ_{Hlim}, Z_{NT}, Z_{L}, Z_{v}, Z_{R}, Z_{W}, and Z_{X} are fatigue strength calculation factors in $\overline{\boldsymbol{X}}_3$.

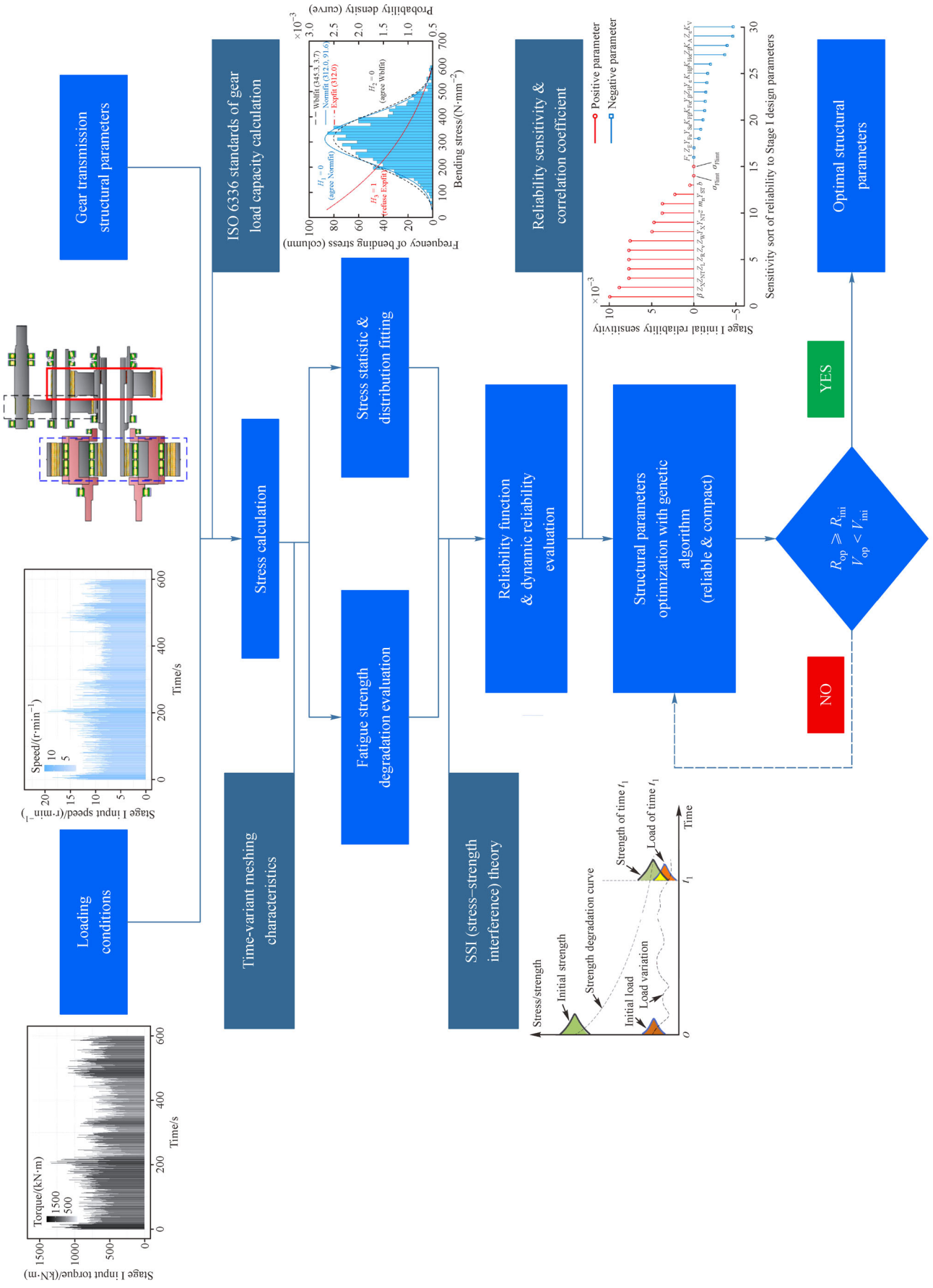

Fig. 1 Flow chart of optimization based on dynamic reliability sensitivity. Normfit, Wblfit, and Expfit represent normal, Weibull, and exponential distributions, respectively.

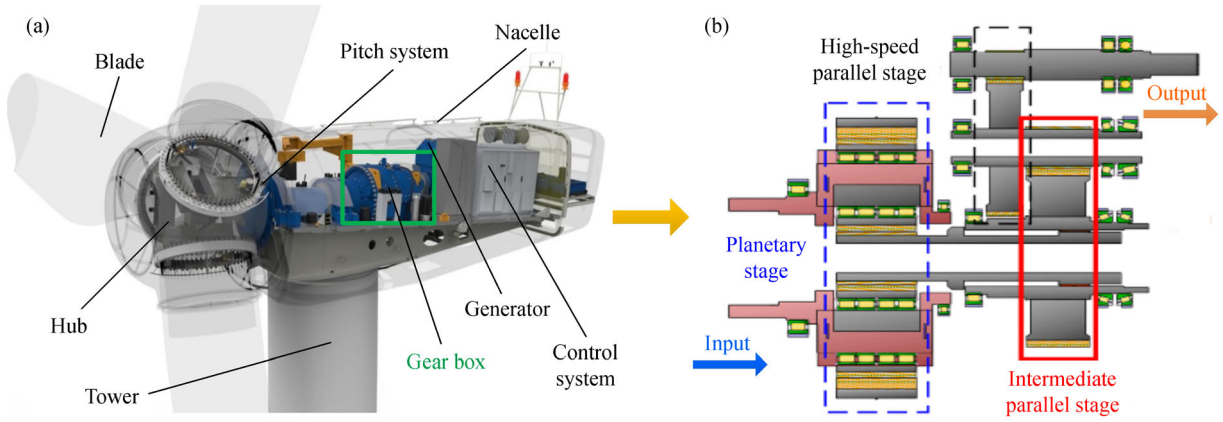

Fig. 2 Schematic of a 2 MW wind turbine gear transmission [29,30].

Table 1 Main structural parameters of the transmission

Gear	Teeth number	Normal module/mm	Pressure angle/(°)	Helix angle/(°)	Gear face width/mm	Shifting coefficient
r^{I}	96	15	25	8	395	–0.2705
p_i^{I} (input)	37	15	25	8	390	0.3924
s^{I}	21	15	25	8	395	0.0000
g_1^{II}	97	11	20	10	310	0.0047
g_2^{II}	23	11	20	10	320	0.0700
g_1^{III}	103	8	20	10	180	0.0240
g_2^{III} (output)	21	8	20	10	190	0.0200

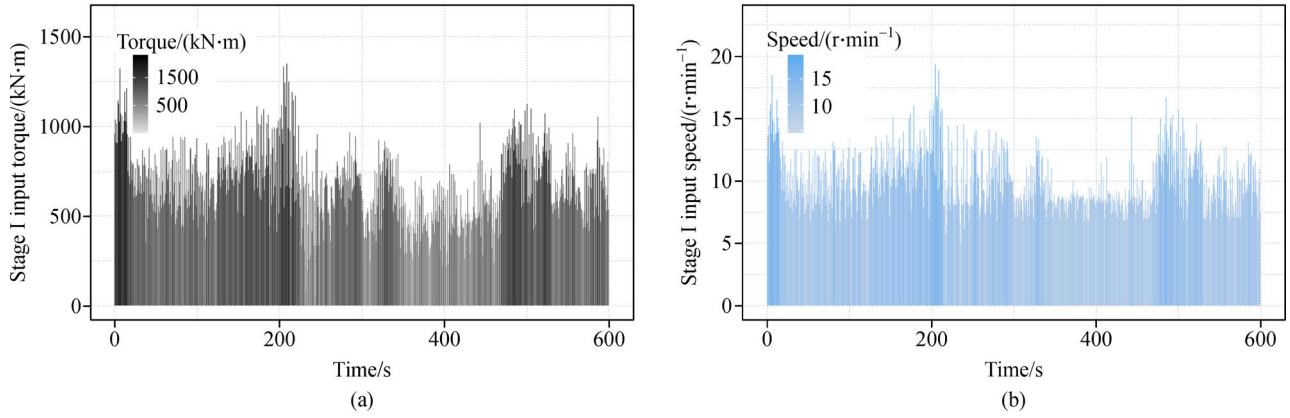

Fig. 3 Input (a) torque and (b) speed history of Stage I within a test time of 600 s.

When SSI theory is applied to evaluate dynamic fatigue reliability, the statistical characteristics of gear stresses should be determined first. A stress statistic method that considers the teeth engaging process was used to identify characteristics in a tractor transmission system in Ref. [17]. Here, Stages I and II are selected to illustrate this method for finding stress characteristics in a wind turbine gear transmission. Figure 4 shows the torque and speed change at Stage I. As displayed in Fig. 4, input torque and input speed are assumed to be constant in one time interval.

The processes of meshing and stress change are shown in Figs. 5(a) and 5(b). As displayed in Fig. 5(a), gears s^{I} and r^{I} in Stage I have finished the meshing process of the first tooth z_2 but failed to complete that of the second tooth z_2 while the torque and speed change (1.0–1.1 s to 1.1–1.2 s time interval). Several explanations are given as follows:

1) If any tooth experiences two time intervals, then it belongs to the time interval with greater stress. As displayed in Fig. 5(a), the second tooth z_2 of gear r^{I} in Stage I belongs to the 1.0–1.1 s time interval when

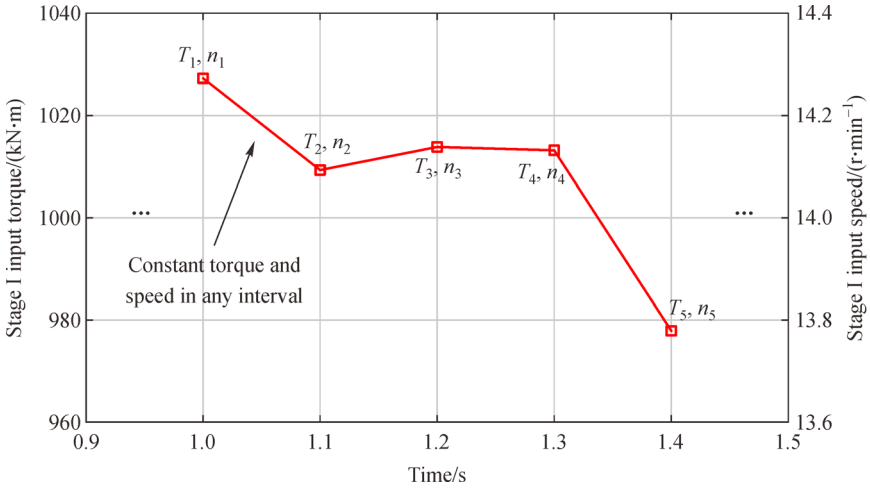

Fig. 4 Changes in input torque and speed at Stage I.

finishing the meshing process between the 1.0–1.1 s and 1.1–1.2 s time intervals. The fifth tooth z_5 of gear s^I in Stage I belongs to the 1.2–1.3 s time interval.

2) The larger torque is taken as the statistical torque for the stress calculation in any time interval. As displayed in Figs. 5(a) and 5(b), the first tooth z_1 that belongs to the 1.1–1.2 s time interval of gear s^I in Stage I takes T_1 as the statistical torque for stress calculation. The first tooth g_1^1 to the eighth tooth g_1^8 of g_1^{II} gear in Stage II take T_1 as the statistical torque for stress calculation as well.

3) The input torque and speed in any time interval are assumed constant.

The provided load history of 600 s represents a limited span of the random loading conditions, given that the service time of a wind turbine needs to be at least 20 years in engineering practice [4,40]. Obtaining statistical loading characteristics within the entire operation time from the given limited loading history is a serious concern. Distribution fitting is one of the effective methods to address this issue. Several classical probability statistical functions, such as lognormal and Weibull distribution, are commonly used for the distribution fitting of fatigue life. Figure 6 shows the bending stress distribution fitting process of the first tooth z_1 from gear g_1^{II} in Stage II. Several explanations describing the process are provided as follows:

1) Tooth stress data are fitted using normal (Normfit), Weibull (Wblfit), and exponential (Expfit) distributions. The goodness of fit is tested with the K–S test method (H = 0 refers to the acceptance of this distribution and H = 1 means rejection; the confidence level is 0.01).

2) Taking the generality of the normal distribution into consideration, it is considered the first choice if it passes the K–S hypothesis test.

3) In accordance with the weakness part principle [41], the distribution of tooth stress with the largest mean value is selected to represent the stress distribution of the gear.

The representative teeth of gears with the largest stress mean value are identified. The stress distributions of gears roughly follow the normal distribution. The p values of distribution fitting differ from one another due to the different stress history of each tooth. The distribution conditions of gears are listed in Table 2.

After stress statistic calculation, fatigue strength degradation is estimated based on residual strength theory. The theory, which was proposed by Schaff and Davidson [37] and extended in Refs. [35,42], is utilized for the fatigue strength degradation estimation of gears. Given the continuous damage, the relationship between residual fatigue strength r and loading cycle n can be defined as

$$r(n) = r(0) - [r(0) - S_{\max}]\left(\frac{n}{N_f}\right)^{C_0}, \tag{7}$$

where $r(n)$ is the residual fatigue strength of the gear under n loading cycles with the unit of N/mm^2, $r(0)$ is the initial fatigue strength of the gear without any damage determined by the ISO 6336-5 standard with the unit of N/mm^2 [43], $S_{\max}$ is the equivalent peak load of the gear with the unit of N/mm^2, n is the number of loading cycles, N_f is the fatigue life of the gear under the equivalent peak load, and C_0 is the degradation factor related to the material property (C_0 equals 1 in this work) [35]. Notably, residual fatigue strength decreases with the increase in loading cycles.

Reliability index calculation based on SSI theory has been clearly described in Refs. [6,33,35,42]. Dynamic fatigue reliability can be defined as the probability that the residual fatigue strength $r(t)$ of the gear is greater than the stress $s(t)$. Dynamic fatigue reliability function $g(t)$ and reliability index $\beta(t)$ can be expressed as

$$g(t) = r(t) - s(t), \tag{8}$$

$$\beta(t) = \frac{\mu_{g(t)}}{\sigma_{g(t)}} = \frac{E[g(t)]}{\sqrt{\mathrm{var}[g(t)]}}, \tag{9}$$

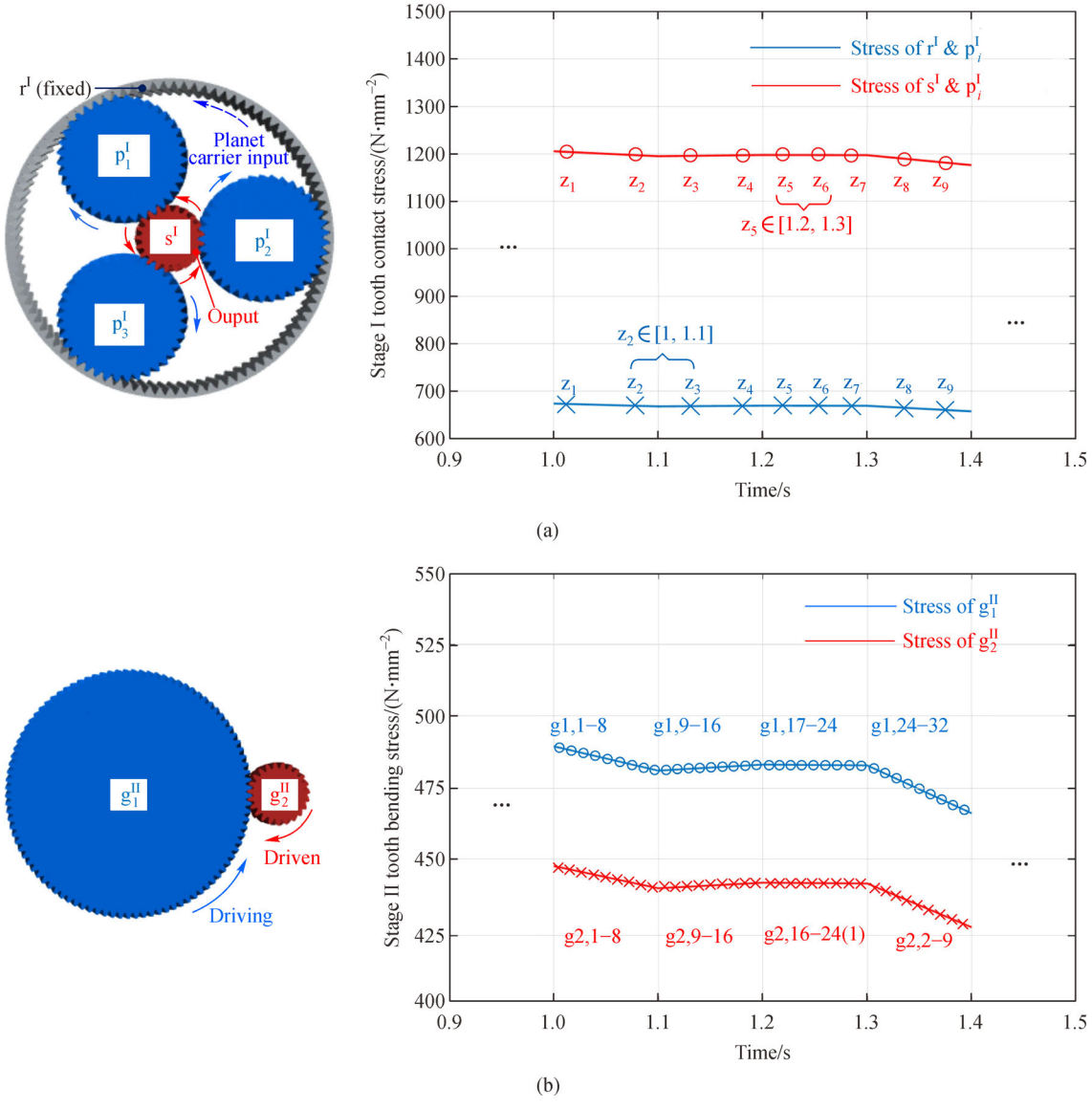

Fig. 5 Gear rotation direction and change in tooth contact and bending stresses at (a) Stage I and (b) Stage II.

where $\beta(t)$ is the fatigue reliability index, $\mu_{g(t)}$ is the mean value of $g(t)$, and $\sigma_{g(t)}$ is the variance of $g(t)$.

If stress and strength are assumed to follow the normal distribution, then dynamic reliability can be calculated as

$$R(t) = \Phi\Big(\beta(t)\Big) = p\{r(t)>s(t)\},\ t \in [0,\ t], \tag{10}$$

where $R(t)$ is the dynamic fatigue reliability, $\Phi(\cdot)$ is the cumulative distribution function of the standard normal distribution, and t is the service time of the component in years.

The serial system concept is generally accepted in many gear transmission reliability studies [6,33,35]. The reliabilities based on the concept, except for planetary gears in the gear transmission, can be calculated as

$$R^i(t) = R^i_{\mathrm{H}}(t)\cdot R^i_{\mathrm{F}}(t), \tag{11}$$

where $R^i(t)$ is the dynamic fatigue reliabilities at Stages II and III, and $R^i_{\mathrm{H}}(t)$ and $R^i_{\mathrm{F}}(t)$ refer to the dynamic contact and bending fatigue reliabilities of Stages II and III, respectively (i = II, III).

The planetary gear train of a wind turbine fails when any planet shows bending fatigue failure or all planets show contact fatigue failure [33]. The dynamic fatigue reliability of Stage I can be calculated as

$$R^{\mathrm{I}}(t) = R^{\mathrm{I}}_{\mathrm{Hr}}(t)\cdot R^{I}_{\mathrm{Fr}}(t)\cdot R^{I}_{\mathrm{Hs}}(t)\cdot R^{I}_{\mathrm{Fs}}(t) \cdot\left[1-\prod_{i=1}^{3}\left(1-R^{\mathrm{I}}_{\mathrm{Hp}i}(t)\right)\right]\cdot\prod_{i=1}^{3}R^{\mathrm{I}}_{\mathrm{Fp}i}(t), \tag{12}$$

where $R^{\mathrm{I}}(t)$ is the dynamic fatigue reliability of Stage I, $R^{\mathrm{I}}_{\mathrm{Hr}}(t)$ and $R^{\mathrm{I}}_{\mathrm{Fr}}(t)$ are the dynamic contact and bending

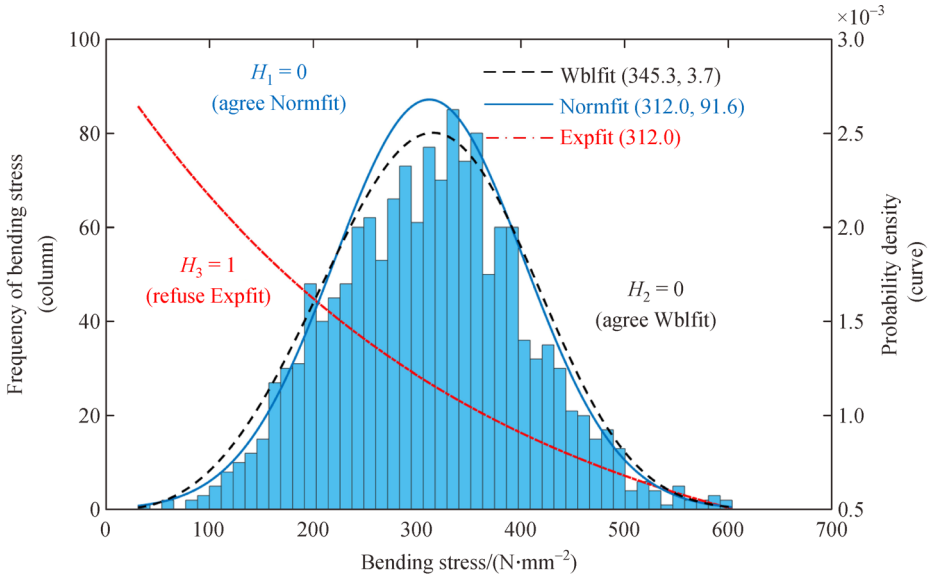

Fig. 6 Distribution fitting of tooth bending stress fitted using normal (Normfit), Weibull (Wblfit), and exponential (Expfit) distributions.

Table 2 Stress distribution fitting conditions of representative teeth of gears

Gear	Tooth	Distribution type of bending stress	Bending stress distribution parameters/(N·mm^{-2})	Test value p_1	Distribution type of contact stress	Contact stress distribution parameters/(N·mm^{-2})	Test value p_2
r^{I}	z_{92}	Normal	(231.53, 67.87)	0.87	Normal	(587.33, 56.34)	0.90
p_i^{I}	z_4	Normal	(359.42, 105.40)	0.65	Normal	(1052.25, 99.21)	0.80
s^{I}	z_1	Normal	(319.76, 91.95)	0.76	Normal	(984.01, 93.62)	0.84
g_1^{II}	z_{44}	Normal	(342.72, 97.76)	0.93	Normal	(956.35, 123.18)	0.42
g_2^{II}	z_{19}	Normal	(311.66, 91.52)	0.54	Normal	(979.59, 100.90)	0.59
g_1^{III}	z_{78}	Normal	(278.87, 82.19)	0.60	Normal	(908.80, 94.88)	0.79
g_2^{III}	z_2	Normal	(275.42, 81.28)	0.02	Normal	(919.09, 113.45)	0.03

fatigue reliabilities of the ring gear in Stage I, respectively, $R_{\mathrm{Hs}}^{\mathrm{I}}(t)$ and $R_{\mathrm{Fs}}^{\mathrm{I}}(t)$ are the dynamic contact and bending fatigue reliabilities of the sun gear in Stage I, respectively, and $R_{\mathrm{Hp}i}^{\mathrm{I}}(t)$ and $R_{\mathrm{Fp}i}^{\mathrm{I}}(t)$ are the dynamic contact and bending fatigue reliabilities of the planetary gears in Stage I, respectively ($i = 1, 2, 3$).

The dynamic fatigue reliability of the gear transmission can be calculated as

$$R(t) = R^{\mathrm{I}}(t) \cdot R^{\mathrm{II}}(t) \cdot R^{\mathrm{III}}(t), \tag{13}$$

where $R^{\mathrm{I}}(t)$, $R^{\mathrm{II}}(t)$, and $R^{\mathrm{III}}(t)$ are the dynamic fatigue reliabilities of the three gear stages.

Distribution fitting and reliability function establishment are based on several hypotheses, such as normal distribution. To evaluate the acceptable level of the reliability results, a numerical solution based on the Monte-Carlo (MC) method is utilized for the verification of dynamic fatigue reliability. The verification process is described as follows:

1) In accordance with the statistical characteristics of the torque loading history shown in Fig. 3(a), 20000 random loading points are sampled with the MC method to form random loading set $\boldsymbol{A}_i$ ($i = 1, 2, ..., 25$). A similar process is implemented to form random residual fatigue strength set $\boldsymbol{B}_i$ ($i = 1, 2, ..., 25$) on the basis of residual fatigue strength $r(n)$.

2) MC-based reliability $\boldsymbol{R}_i^M$ ($i = 1, 2, ..., 25$) is obtained by comparing loading set $\boldsymbol{A}_i$ and fatigue strength set $\boldsymbol{B}_i$. The numerical solution is then compared with the analytical solution shown in Eqs. (8) and (9) to estimate the relative error.

2.3 Reliability sensitivity estimation

Compared with traditional reliability sensitivity, dynamic fatigue reliability sensitivity can be explained as the effects of changes in loading conditions, material properties, design parameters, and other variables on dynamic fatigue reliability during operation. Many scholars used sensitivity to discuss the effects of design parameter changes under random loading conditions on reliability [14,33,44]. On the

basis of the first-order second moment and gear transmission reliability sensitivity estimation methods in Refs. [14,33], dynamic fatigue reliability sensitivity can be calculated as follows:

$$\frac{\mathrm{d}R(t)}{\mathrm{d}\left(\overline{\boldsymbol{X}},\ t\right)^{\mathrm{T}}}=\frac{\partial R\left(\beta(t)\right)}{\partial\beta(t)}\frac{\partial\beta(t)}{\partial u_{g(t)}}\frac{\partial u_{g(t)}}{\partial\left(\overline{\boldsymbol{X}},t\right)^{\mathrm{T}}}+\frac{\partial R\left(\beta(t)\right)}{\partial\beta(t)}\frac{\partial\beta(t)}{\partial\sigma_{g(t)}}\frac{\partial\sigma_{g(t)}}{\partial\left(\overline{\boldsymbol{X}},t\right)^{\mathrm{T}}},\tag{14}$$

$$\frac{\partial R\left(\beta(t)\right)}{\partial\beta(t)}=\varphi\left(\beta(t)\right),\tag{15}$$

$$\frac{\partial\beta(t)}{\partial u_{g(t)}}=\frac{1}{\sigma_{\mu(t)}},\tag{16}$$

$$\frac{\partial u_{g(t)}}{\partial\left(\overline{\boldsymbol{X}},t\right)^{\mathrm{T}}}=\left[\frac{\partial\overline{g}}{\partial\boldsymbol{X}_1},\ \frac{\partial\overline{g}}{\partial\boldsymbol{X}_2},\ \ldots,\ \frac{\partial\overline{g}}{\partial\boldsymbol{X}_n}\right],\tag{17}$$

$$\frac{\partial\beta(t)}{\partial\sigma_{g(t)}}=-\frac{u_{g(t)}}{\sigma^2_{\mu(t)}},\tag{18}$$

$$\frac{\partial\sigma_{g(t)}}{\partial\left(\overline{\boldsymbol{X}},t\right)^{\mathrm{T}}}=\frac{1}{2\sigma_{g(t)}}\left[\frac{\partial\overline{g}}{\partial\boldsymbol{X}}\otimes\frac{\partial\overline{g}}{\partial\boldsymbol{X}}\right],\tag{19}$$

where $\varphi\left(\beta(t)\right)$ is the probability density function of standard normal distribution, and $\otimes$ is the Kronecker product.

The relationship among the initial design parameters can be described by the correlation coefficient. The correlation coefficients of the initial design parameters can be calculated as

$$\rho(\boldsymbol{X}_1,\boldsymbol{X}_2)=\frac{\mathrm{Cov}(\boldsymbol{X}_1,\boldsymbol{X}_2)}{\sqrt{\mathrm{Var}(\boldsymbol{X}_1)\mathrm{Var}(\boldsymbol{X}_2)}},\tag{20}$$

where $\rho(\boldsymbol{X}_1,\boldsymbol{X}_2)$ is the correlation coefficient between two initial design parameters $\boldsymbol{X}_1$ and $\boldsymbol{X}_2$, and $\mathrm{Cov}(\boldsymbol{X}_1,\boldsymbol{X}_2)$ is the covariance between parameters $\boldsymbol{X}_1$ and $\boldsymbol{X}_2$ ($\boldsymbol{X}_1,\ \boldsymbol{X}_2\in\overline{\boldsymbol{X}}$).

Given the large number of initial design parameters, cluster analysis based on the acquired correlation coefficients is performed for the classification of such parameters into several groups. The design variables are then determined based on these groups. The correlation coefficient distance is a good reference to distinguish the groups of design parameters. The similarity degree can be calculated by the correlation distance and is expressed as

$$d(\boldsymbol{X}_1,\ \boldsymbol{X}_2)=2-\rho(\boldsymbol{X}_1,\ \boldsymbol{X}_2),\tag{21}$$

where $d(\boldsymbol{X}_1,\boldsymbol{X}_2)$ is the similarity degree, and its potential fluctuation range lies within 1 to 2.

2.4 Optimization design

The design variables to be optimized are tooth number Z, normal module m_{n}, face width b, and helix angle β from the reliability sensitivity results. The set of design variables can be described as follows:

$$\begin{aligned}\overline{\boldsymbol{x}}&=[Z_1,Z_2,Z_3,Z_4,Z_5,Z_6,Z_7,m_{\mathrm{n1}},m_{\mathrm{n2}},m_{\mathrm{n3}},b_1,b_2,b_3,\beta_1,\beta_2,\beta_3]^{\mathrm{T}}\\&=[x_1,x_2,x_3,x_4,x_5,x_6,x_7,x_8,x_9,x_{10},x_{11},x_{12},x_{13},x_{14},x_{15},x_{16}]^{\mathrm{T}},\end{aligned}\tag{22}$$

where Z_1, Z_2, and Z_3 are the tooth number of gears in Stage I, Z_4 and Z_5 are the tooth number of gears in Stage II, Z_6 and Z_7 are the tooth number of gears in Stage III, m_{n1}, m_{n2}, and m_{n3} are the normal modules of the three stages, b_1, b_2, and b_3 are the face widths of the three stages, and β_1, β_2, and β_3 are the helix angles of the three stages.

The optimization function toward the minimum volume of the wind turbine gear transmission structural parameters can be described as

$$\min F(x)=\frac{\pi x_8^2x_{11}}{4\cos^2x_{14}}x_1^2+\frac{\pi x_9^2x_{12}}{4\cos^2x_{15}}(x_4^2+x_5^2)+\frac{\pi x_{10}^2x_{13}}{4\cos^2x_{16}}(x_6^2+x_7^2).\tag{23}$$

The constraint conditions of dynamic fatigue reliability include the gear transmission basic constraint, the static strength constraint, and the sensitivity constraint. For the gear transmission basic constraint, the fatigue reliability of the gear transmission structure should be greater than 99% in five years and greater than 95% in 10 years. The fatigue reliability of the optimized structure should be greater than that of the initial structure [6,33,42]. The volume of the optimized structure should be smaller than that of the initial structure [6,33,42]. For the static strength constraint, bending and contact static allowable strength should be greater than the maximum bending and contact stress. For the sensitivity constraint, the transmission ratio of Stage I should be limited within 5.5 to 6. The transmission ratio of Stages II and III should be limited within 4.2 to 5. The overall transmission ratio should be limited within 114 to 116. Helix angle β should be limited within 8° to 15° and satisfy the transmission requirement [23].

In accordance with the reliability sensitivity results, lubrication factor Z_{L}, velocity factor Z_{v}, and zone factor Z_{H} are selected to establish the reliability sensitivity constraints.

Increments in lubrication factor Z_{L} and velocity factor Z_{v} exert a positive effect on fatigue reliability due to the positive value of reliability sensitivity. Circumferential velocity v ($v=\pi dn/60000$) is selected to control the value

of lubrication factor Z_L and velocity factor Z_v. The transmission structure with a larger value of the normal module and a higher transmission ratio is selected to increase the value of the two factors. However, the fatigue reliability decreases, and the value of zone factor Z_H ($Z_H = \sqrt{2\cos\beta_b \cos\alpha_t' / (\cos^2\alpha_t \sin\alpha_t')}$) increases. Here, β_b ($\beta_b = \arctan(\tan\alpha_n / \cos\beta)$), α_t' ($\text{inv}\alpha_t' = \text{inv}\alpha_t + 2(x_1 \pm x_2)/(Z_1 + Z_2)$), and α_t ($\alpha_t = \arctan(\tan\alpha_t / \cos\beta)$) are used in the calculation of zone factors, and the transmission structure with a higher helix angle β is chosen to control the value of zone factor Z_H.

Then, the dynamic fatigue reliability constraints can be described as the following inequality:

$$\begin{cases} R_s^{op}(5) \geqslant 99.5\%, \\ R_s^{op}(10) \geqslant 95.0\%, \\ R_s^{op}(t) \geqslant R_s^{ini}(t), \\ V_{op} < V_{ini}, \\ \sigma_{Fpst} > \sigma_{Fst}, \\ \sigma_{Hpst} > \sigma_{Hst}, \\ 5.5 \leqslant Z_1/Z_3 + 1 \leqslant 6, \\ 4.2 \leqslant Z_7/Z_8 \leqslant 5, \\ 4.2 \leqslant Z_{12}/Z_{13} \leqslant 5, \\ 114 \leqslant i_{StgI} i_{StgII} i_{StgIII} \leqslant 116, \\ 8 \leqslant \beta_1 \leqslant \beta_2 \leqslant \beta_3 \leqslant 15, \\ 0.6\pi m_n - b\sin\beta \leqslant 0. \end{cases} \tag{24}$$

where R_s^{op} is the fatigue reliability of optimized gear transmission, R_s^{ini} is the fatigue reliability of initial gear transmission, σ_{Fpst} and σ_{Hpst} are maximum bending and contact static allowable strength, σ_{Fst} and σ_{Hst} are the maximum bending and contact stress, and i_{StgI}, i_{StgII} and i_{StgIII} are the transmission ration of stages.

Figure 7 shows the main procedures of the genetic algorithm. The design variable, the design variable set, and all the sets represent a gene, an individual, and the population, respectively. A new individual is created by exchanging the corresponding gene, which is selected randomly, between two adjacent individuals. When a new individual is generated, every gene has the mutation probability (η = 0.025) to change randomly. The new population, with the number of individuals reaching 100, consists of the offspring (including mutation offspring) and fraction parents with high fitness. The convergence accuracy (CA) value is 0.001.

3 Results and discussions

3.1 Dynamic fatigue reliability

The allowable bending and contact stresses of 18Crnimo7–6 gears are 550 and 1425 N/mm^2, respectively, and those for the 42CrMo gear are 350 and 850 N/mm^2, respectively, according to Ref. [43]. The initial fatigue reliabilities (R_{F0} and R_{H0}) and safety factors (S_F and S_H) of gears are shown in Table 3. As displayed in Table 3, the gears in the three stages have high initial reliabilities and safety factors. The model-based reliabilities (second and third columns in

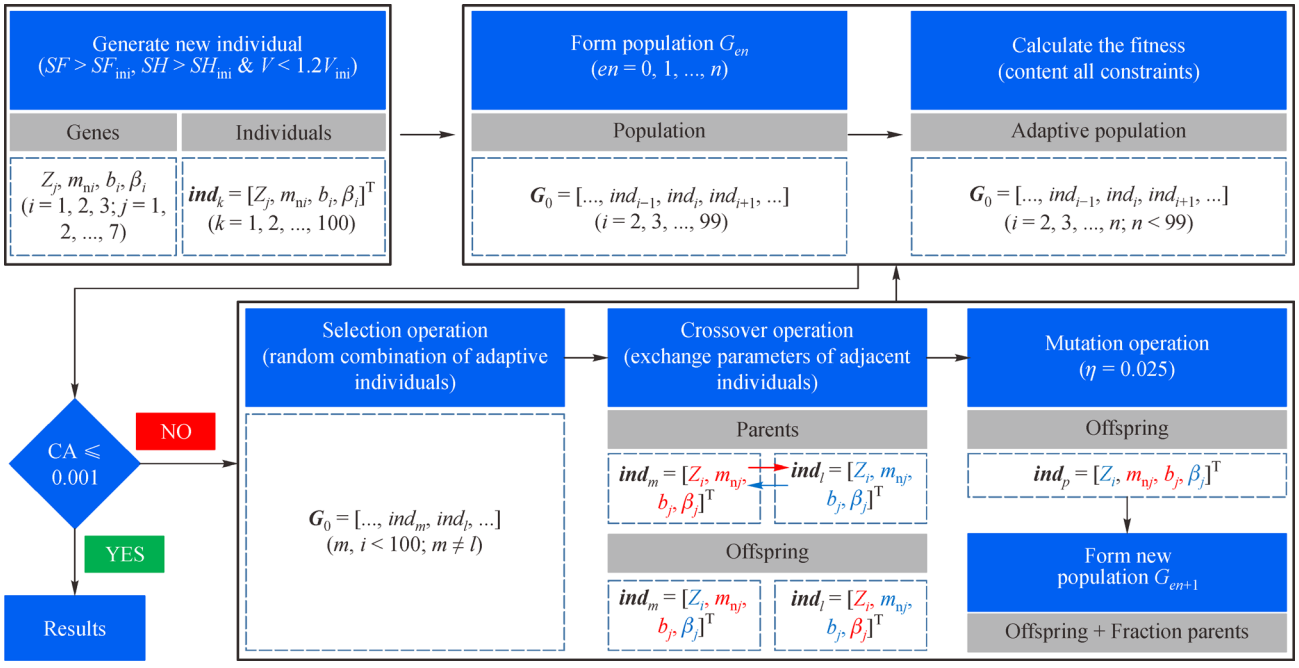

Fig. 7 Flow chart of the genetic algorithm of gear transmission optimization.

Table 3 Initial reliabilities and safety factors

Gear	R_{F0}/%	R_{H0}/%	S_F [a)]	S_H [b)]
r^I	99.9785	99.9923	1.90	1.53
p_i^I	99.9934	99.9922	2.01	1.52
s^I	99.9992	99.9988	2.10	1.61
g_1^{II}	99.9993	99.9990	2.11	1.64
g_2^{II}	99.9998	99.9986	2.14	1.60
g_1^{III}	99.9999	99.9999	2.34	1.77
g_2^{III}	99.9999	99.9999	2.37	1.75

Note: [a)] $S_F > 2.00$ is very high ($R_{SF} > 99.99\%$), $S_F > 1.60$ is high ($R_{SF} > 99.90\%$), and $S_F > 1.25$ is general ($R_{SF} > 99.00\%$); [b)] $S_H > 1.50$ is very high ($R_{SH} > 99.99\%$), $S_H > 1.25$ is high ($R_{SH} > 99.90\%$), and $S_H > 1.00$ is general ($R_{SH} > 99.00\%$).

Table 3) and the reliabilities determined by the safety factor (R_{SF} and R_{SH}) show that the two initial reliability results agree with each other.

The dynamic fatigue reliabilities calculated by Eqs. (7)–(10) and the MC-based reliabilities of the three stages are shown in Fig. 8. A decrease in the reliabilities is observed as the operating time increases. The dynamic bending fatigue reliabilities are shown in Fig. 8(a). The bending fatigue reliability of Stage III decreases more remarkably than that of Stages II and I. This result is attributed to the higher rotational speed encountered by Stage III. The bending fatigue reliability of Stage I is slightly lower than that of Stage II due to the former's higher bending stress. The dynamic contact fatigue reliabilities are shown in Fig. 8(b). The contact fatigue reliability of Stage III decreases more remarkably than that of Stages II and I. This result is due to the rapid degradation of contact fatigue strength under the numerous loading cycles. According to the two dynamic fatigue reliabilities, after 25 years of operation, Stage III will have high failure probabilities (0.1931 and 0.3051 for bending fatigue fracture and contact fatigue failure, respectively) and can be regarded as the key stage to be optimized in this transmission. The results of the comparison between bending and contact fatigue reliabilities are shown in Fig. 8(c). They show that the bending fatigue reliabilities of stages are higher than the contact fatigue reliabilities. This result is attributed to the large module feature of the gear ($m_n \geqslant 8$ mm). The dynamic fatigue reliabilities and MC-based reliabilities of three stages are shown in Fig. 8(d). The fatigue reliability of Stage III decreases more markedly compared with that in Stages I and II. The relative error of Stage I is the smallest

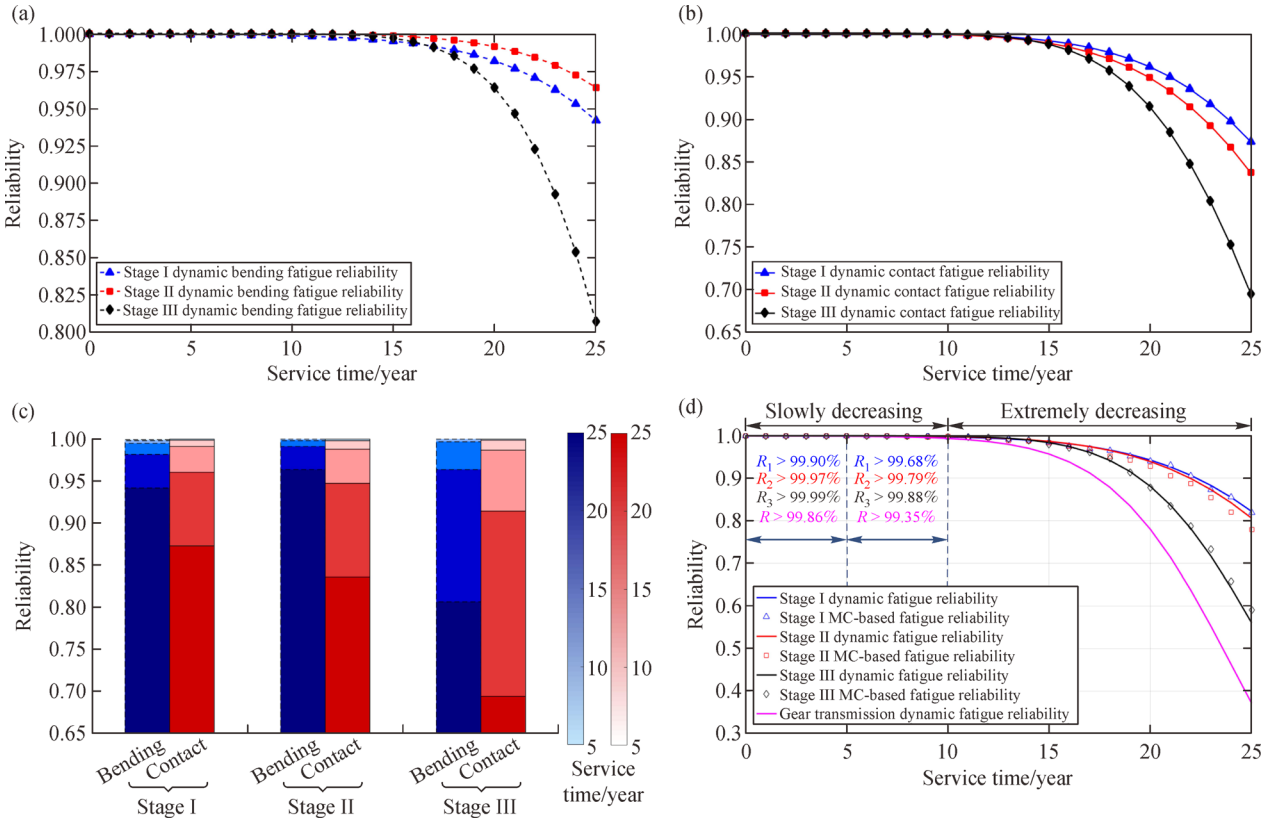

Fig. 8 Dynamic fatigue reliabilities of the three stages: (a) Dynamic bending fatigue reliabilities of the stages; (b) dynamic contact fatigue reliabilities of the stages; (c) comparison of the two types of fatigue reliability of the stages; and (d) dynamic fatigue reliabilities of the stages and gear transmission.

(1.18%), followed by those of Stages II (3.37%) and III (5.19%). This finding illustrates that the model has acceptable accuracy in the reliability evaluation. The service time can be divided into the first period (0–10 years) and the last period (10–25 years) depending on the decrease rate of the fatigue reliabilities. In the first period, the fatigue reliabilities of the three gear stages decreases slightly, but they decrease remarkably in the last period. The actual failure conditions of this gear transmission may differ from the results due to the disregard of assembly errors, manufacturing errors, extreme loads, and other variables in the model.

3.2 Reliability sensitivity

Reliability sensitivity can directly reflect the effects of the change in design parameters on reliability. The initial fatigue reliability sensitivities of the three stages are shown in Fig. 9. The parameters with positive sensitivity values are marked as the red column, and the blue column contains the negative parameters. Fatigue reliability achieves positive feedback as the values of the positive parameters increase but decrease with the increase in negative parameters. The sensitivity values of the initial design parameters vary from one another due to the different effects on reliability. The sensitivities of the parameters in Stage I are shown in Fig. 9(a). Fatigue reliability is highly sensitive to the change in helix angle (β), followed by the size factor of contact fatigue strength calculation (Z_X) and the dynamic factor (K_V). Fatigue reliability is the most insensitive to tangential tooth load (F_t), followed by contact allowable stress (σ_{Hlim}) and bending allowable stress (σ_{Flim}). The sensitivities of the parameters in Stages II and III are shown in Figs. 9(b) and 9(c), respectively. The same trend of sensitivity values is observed in Stages II and III. This observation is attributed to the similar main failure of gears in the three stages.

The initial reliability sensitivities of the three stages only represent the effects of the change in design parameters in the initial time. The dynamic sensitivities of the parameters are shown in Fig. 10. An increase in sensitivity is observed as the operating time increases. However, the tangential tooth load (F_t) and allowable stresses (σ_{Hlim} and σ_{Flim}) with sort numbers 16, 15, and 14 have a small effect on reliability during operation. The tangential tooth load (F_t) and allowable stress (σ_{Hlim} and σ_{Flim}) are excluded from the initial design parameter set $\overline{\boldsymbol{X}}$ due to their slight effects on reliability.

The correlation coefficient matrix reflects the correlation of the parameters directly. The correlation coefficient matrix of the initial design parameters is shown in Fig. 11. Several parameters, such as life calculation factors (Z_{NT} and Y_{NT}), roughness factor (Z_R), working hardness factor (Z_W), application factor (K_A), elasticity factor (Z_E), and bending stress correlation factor (Y_{ST}), are unsuitable as design variables because of their low correlation with the other parameters. These parameters are determined by the design requirement, machining accuracy, application condition, and other factors and are difficult to change. These parameters are excluded from the initial design parameters set $\overline{\boldsymbol{X}}$.

A cluster dendrogram flow of the remaining 20 initial design parameters is shown in Fig. 12. According to the similarity degree of parameters, these parameters can be roughly divided into four groups, three of which are highly affected by helix angle (β), normal module (m_n), and face width (b). The remaining parameters are categorized under the fourth group. Helix angle (β), number of teeth (Z), gear modulus (m_n), and face width (b) are selected as the design variables due to their representativeness of such parameters. However, other parameters, such as lubrication factor (Z_L), velocity factor (Z_v), and zone factor (Z_H), exert a valuable effect on reliability and are thus used as sensitivity constraints.

3.3 Parameter optimization

The genetic algorithm compiled by the Matlab software is used to search for the optimized structural parameters of the gear transmission. The parameters of the initial and optimized structures are shown in Table 4. The volume of the initial structure is 1.0681 m^3, but it decreases to 1.0299 m^3 (3.58% reduction) after optimization.

The dynamic fatigue reliabilities of the optimized structure are shown in Fig. 13. Compared with the reliabilities in Fig. 8(d), the reliabilities of Stage III and the gear transmission increase remarkably, but only a slight change occurs in Stages I and II. The maximum reliability changes of Stages I to III after 25 years of operation are 1.45%, –1.99%, and 15.1%, respectively.

The comparison of the reliability of the initial and optimized structures is shown in Table 5. The fatigue reliability of the optimized structure is increased, and the maximum increase can reach 9.65% after 25 years of operation.

The optimization effect can be defined as the value of the dynamic fatigue reliability of the optimized structure divided by that of the initial one. The effects in the three stages and gear transmission are shown in Fig. 14. Stage III with a maximum optimization effect coefficient of 1.27 and Stage I with a maximum of 1.02 are optimized ideally, whereas Stage II with the smallest value of 0.97 fails to show improved reliability. However, the fatigue reliability of the optimized structure is improved, with a maximum optimization effect coefficient of 1.26. This result is primarily attributed to the significant reliability improvement in Stage III and small reliability changes in Stages I and II. The decrease in the transmission ratio and increase in helix angle causes a stress reduction and fatigue reliability improvement in the Stage III gears. The volume

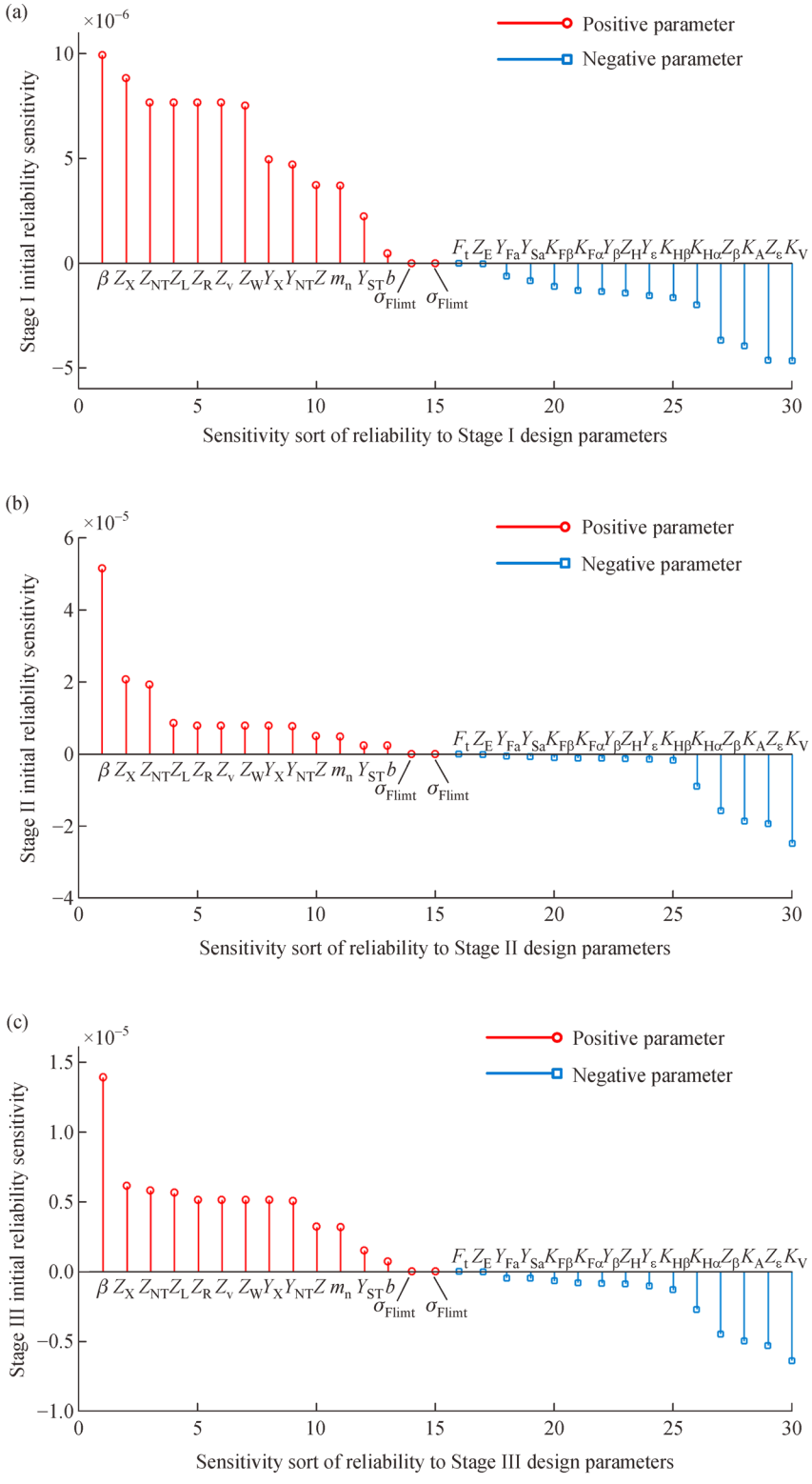

Fig. 9 Initial fatigue reliability sensitivities in the three stages: (a) Stage I, (b) Stage II, and (c) Stage III.

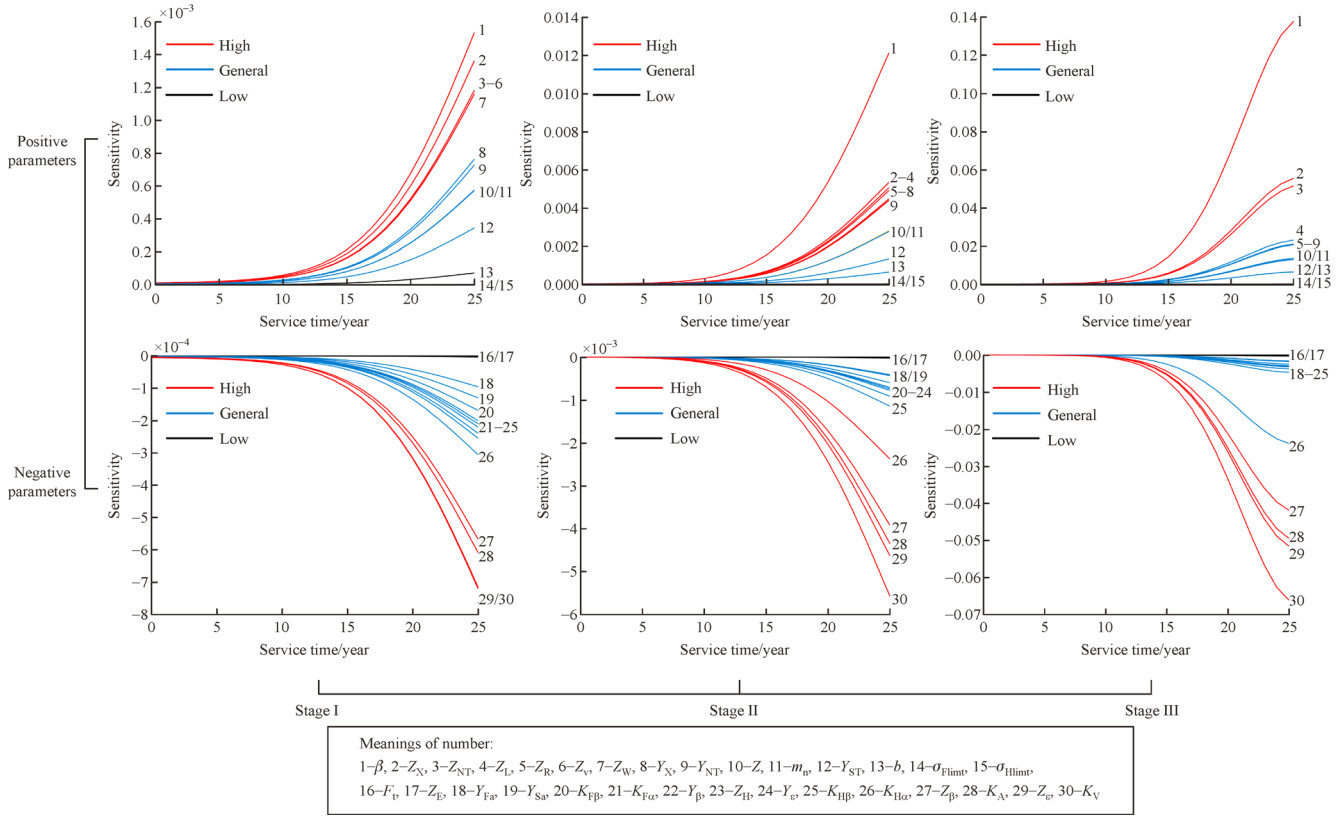

Fig. 10 Dynamic fatigue reliability sensitivities of the three stages.

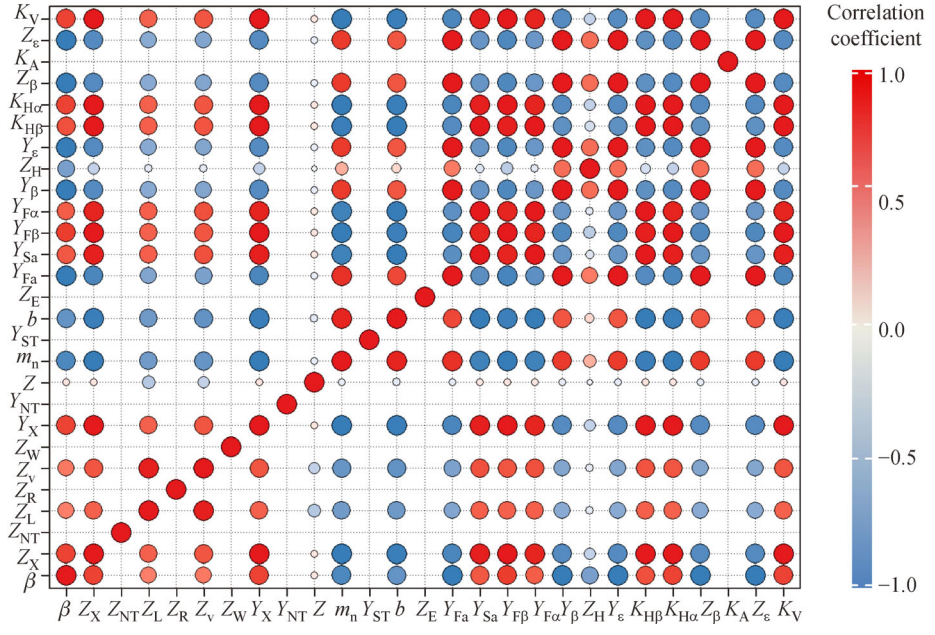

Fig. 11 Correlation coefficient matrix of the initial design parameters.

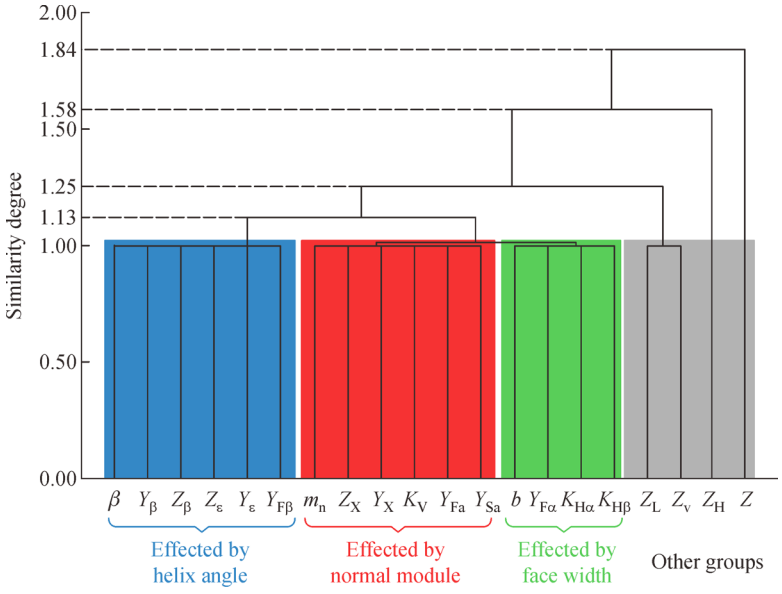

Fig. 12 Cluster dendrogram of design parameters.

Table 4 Structural parameters of the initial gear transmission structure and the optimized one

Gear pairs	Normal module/mm	Tooth number	Helix angle/(°)	Gear face width/mm
Initial Stage I	15	96/37/21	8	390
Initial Stage II	11	97/23	10	320
Initial Stage III	8	103/21	10	190
Optimized Stage I	16	94/37/20	10	350
Optimized Stage II	11	93/21	12	310
Optimized Stage III	8	111/25	12	160

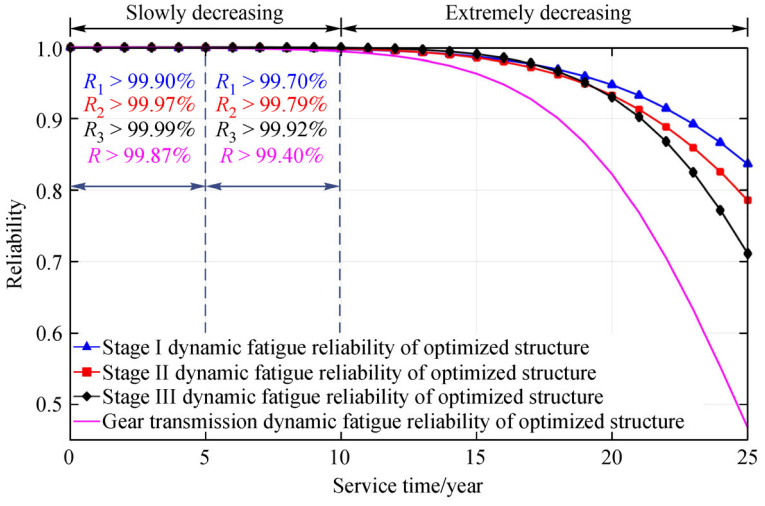

Fig. 13 Dynamic fatigue reliability of the optimized gear transmission.

Table 5 Reliability results for the initial and optimized structures

Service time/year	Reliability/%	
	After optimization	Before optimization
0	99.9460	99.9460
5	99.8741	99.8696
10	99.4026	98.3551
15	96.3191	95.6770
20	82.2016	77.9884
25	46.7794	37.1282

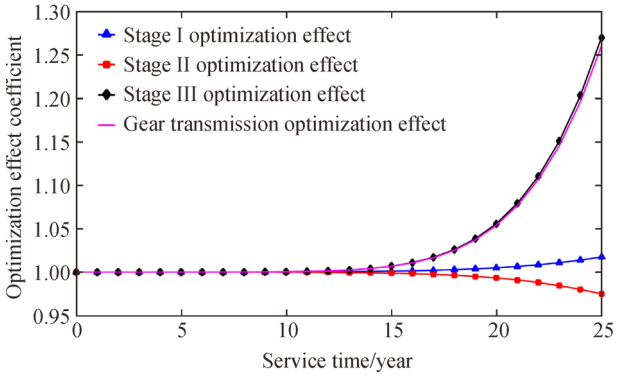

Fig. 14 Optimization effect of the optimization effect of the gear transmission.

decrease in Stages I and II induced by reducing the face width contributes to the volume decrease of gear transmission.

4 Conclusions

This work proposes a novel RBDO model based on dynamic fatigue reliability sensitivity for a wind turbine gear transmission to predict the optimal structural parameters with a reduced volume and ensured reliability. The main conclusions are summarized as follows:

1) In the first period of service time, the fatigue reliabilities of the three gear stages decrease slightly, but they decrease remarkably in the last period. After 25 years of service, Stage III has the lowest reliability value of 56.05%, and Stage I has the highest reliability.

2) The representative parameters that exert a considerable effect on fatigue reliability are helix angle, tooth number, normal module, and face width.

3) The volume of the optimized structure decreases by 3.58%, and its fatigue reliability increases with a maximum value of 9.65%. Stage III has the highest optimization effect with a value of 1.27, and Stage II has the lowest optimization effect.

Acknowledgements This work was financially supported by the National Natural Science Foundation of China (Grant No. U1864210).

Nomenclature

b	Face width, mm
CA	Convergence accuracy
C_0	Degradation factor
d_1	Diameter of the reference circle, mm
$d(\boldsymbol{X}_1,\boldsymbol{X}_2)$	Similarity degree between two design parameters
F_t	Tangential tooth load, N
$g(t)$	Dynamic fatigue reliability function
g_1^1	First tooth of the pinion gear in Stage II
g_1^8	Eighth tooth of the wheel gear in Stage II
g_1^{II}	Wheel gear in Stage II
g_2^{II}	Pinion gear in Stage II
g_1^{III}	Wheel gear in Stage III
g_2^{III}	Pinion gear in Stage III
i_{StgI}	Transmission ration of Stage I
i_{StgII}	Transmission ration of Stage II
i_{StgIII}	Transmission ration of Stage III
K_A	Application factor
$K_{F\beta}$	Face load factor of bending stress calculation
$K_{F\alpha}$	Transverse load factor of bending stress calculation
$K_{H\beta}$	Face load factor of contact stress calculation
$K_{H\alpha}$	Transverse load factor of contact stress calculation
K_V	Dynamic factor
m_n	Normal module, mm
n	Gear velocity
p_i^I	Planetary gear in Stage I
$R(t)$	Dynamic reliability, %
R_{F0}	Initial bending fatigue reliability, %
R_{H0}	Initial contact fatigue reliability, %
R_{SF}	Initial bending fatigue reliability determined by the safety factor, %
R_{SH}	Initial contact fatigue reliability determined by the safety factor, %
R_s^{op}	Fatigue reliability of the optimized structure
R_s^{ini}	Fatigue reliability of the initial structure
$R^i(t)$	Dynamic fatigue reliability of Stages II and III, %
$R_H^i(t)$	Dynamic contact fatigue reliability of Stages II and III, %
$R_F^i(t)$	Dynamic bending fatigue reliability of Stages II and III, %
$R^I(t)$	Dynamic fatigue reliability of Stage I, %
$R_{Fr}^I(t)$	Dynamic bending fatigue reliabilities of the ring gear, %
$R_{Hr}^I(t)$	Dynamic contact fatigue reliabilities of the ring gear, %
$R_{Fs}^I(t)$	Dynamic bending fatigue reliabilities of the sun gear, %
$R_{Hs}^I(t)$	Dynamic contact fatigue reliabilities of the sun gear, %
$R_{Fpi}^I(t)$	Dynamic bending fatigue reliabilities of the planetary gear, %
$R_{Hpi}^I(t)$	Dynamic contact fatigue reliabilities of the planetary gear, %

s^I	Sun gear in Stage I
$r(n)$	Residual fatigue strength of the gear under n loading cycle numbers, N/mm^2
$r(0)$	Initial fatigue strength of the gear without any damage
S_{max}	Equivalent peak load of the gear, N/mm^2
S_F	Initial bending safety factor
S_H	Initial contact safety factor
r^I	Ring gear in Stage I
T_1	Sample torque for stress calculation
t	Service time, year
u	Gear ratio
V_{op}	Volume of the optimized structure, m^3
V_{ini}	Volume of the initial structure, m^3
v	Circumferential velocity, m/s
$\overline{\boldsymbol{X}}_1$	Basic factor set
$\overline{\boldsymbol{X}}_2$	Stress calculation factor set
$\overline{\boldsymbol{X}}_3$	Fatigue strength calculation factor set
$\overline{\boldsymbol{X}}$	Initial design parameter set
$\bar{\boldsymbol{x}}$	Design variable set
Y_{Fa}	Tooth form factor
Y_{Sa}	Dedendum stress concentration factor
Y_ε	Contact ratio factor of bending stress calculation
Y_β	Helix angle factor of bending stress calculation
Y_{ST}	Stress correction factor of bending fatigue strength calculation
Y_{NT}	Life factor of bending fatigue strength calculation
Y_X	Size factor of bending fatigue strength calculation
Z_H	Zone factor
Z_E	Elasticity factor
Z_ε	Contact ratio factor of contact stress calculation
Z_β	Helix angle factor of contact stress calculation
Z_{NT}	Life factor of contact fatigue strength calculation
Z_L	Lubrication factor
Z_v	Velocity factor
Z_R	Roughness factor
Z_W	Work hardening factor
Z_X	Size factor of contact fatigue strength calculation
z_1	First tooth of the ring gear in Stage I
z_2	Second tooth of the ring gear in Stage I
z_5	Fifth tooth of the sun gear in Stage I
α_t	Calculation factor of the zone factor, $\alpha_t = \arctan(\tan\alpha_n/\cos\beta)$
β	Helix angle, °
$\beta(t)$	Reliability index
β_b	Calculation factor of the zone factor, $\beta_b = \arctan(\tan\beta\cos\alpha_t)$
η	Mutation probability
$\mu_{g(t)}$	Mean value of dynamic fatigue reliability
$\rho(\boldsymbol{X}_1,\boldsymbol{X}_2)$	Correction coefficient between two design parameters
σ_F	Bending stress of tooth root, N/mm^2
σ_{Fst}	Maximum bending static strength, N/mm^2
σ_{Fpst}	Maximum bending static allowable strength, N/mm^2
σ_{Flim}	Allowable bending stress number, N/mm^2
σ_H	Contact stress of tooth face, N/mm^2
σ_{Hst}	Maximum contact static strength, N/mm^2
σ_{Fst}	Maximum contact static allowable strength, N/mm^2
σ_{Hlim}	Allowable contact stress number, N/mm^2
$\sigma_{g(t)}$	Variance of dynamic fatigue reliability function
$\Phi(\cdot)$	Cumulative distribution function of the standard normal distribution
$\varphi(\cdot)$	Probability density function of standard normal distribution
$\otimes$	Kronecker product

References

1. He H F, Liu H J, Zhu C C, et al. Study on the gear fatigue behavior considering the effect of residual stress based on the continuum damage approach. Engineering Failure Analysis, 2019, 104: 531–544
2. Zhou Y, Zhu C C, Liu H J. A micropitting study considering rough sliding and mild wear. Coatings, 2019, 9(10): 639
3. Yuan M, Liu Y, Yan D H, et al. Probabilistic fatigue life prediction for concrete bridges using Bayesian inference. Advances in Structural Engineering, 2019, 22(3): 765–778
4. Zhou J, Roshanmanesh S, Hayati F, et al. Improving the reliability of industrial multi-MW wind turbines. Insight–Non-Destructive Testing and Condition Monitoring, 2017, 59(4): 189–195
5. Yi P X, Hu P, Shi T. Numerical analysis and experimental investigation of modal properties for the gearbox in wind turbine. Frontiers of Mechanical Engineering, 2016, 11(4): 388–402
6. Chen H T, Fan J K, Jing S X, et al. Probabilistic design optimization of wind turbine gear transmission system based on dynamic reliability. Journal of Mechanical Science and Technology, 2019, 33(2): 579–589
7. Nejad A R, Gao Z, Moan T. On long-term fatigue damage and reliability analysis of gears under wind loads in offshore wind turbine drivetrains. International Journal of Fatigue, 2014, 61: 116–128
8. Chen H T, Wang X H, Gao H C, et al. Dynamic characteristics of wind turbine gear transmission system with random wind and the effect of random backlash on system stability. Proceedings of the Institution of Mechanical Engineers. Part C, Journal of Mechanical Engineering Science, 2017, 231(14): 2590–2597
9. Zhu S P, Liu Q, Lei Q, et al. Probabilistic fatigue life prediction and reliability assessment of a high pressure turbine disc considering load variations. International Journal of Damage Mechanics, 2018, 27(10): 1569–1588
10. Zhu S P, Liu Q, Peng W W, et al. Computational–experimental approaches for fatigue reliability assessment of turbine bladed disks. International Journal of Mechanical Sciences, 2018, 142–143: 502–517
11. Lu C, Feng Y W, Fei C W. Weighted regression-based extremum

response surface method for structural dynamic fuzzy reliability analysis. Energies, 2019, 12(9): 1588
12. Zhu S P, Liu Q, Zhou J, et al. Fatigue reliability assessment of turbine discs under multi-source uncertainties. Fatigue & Fracture of Engineering Materials & Structures, 2018, 41(6): 1291–1305
13. Mishra S K, Roy B K, Chakraborty S. Reliability-based-design-optimization of base isolated buildings considering stochastic system parameters subjected to random earthquakes. International Journal of Mechanical Sciences, 2013, 75: 123–133
14. Zhou D, Zhang X F, Zhang Y M. Dynamic reliability analysis for planetary gear system in shearer mechanisms. Mechanism and Machine Theory, 2016, 105: 244–259
15. Xie L Y, Wu N X, Qian W X. Time domain series system definition and gear set reliability modeling. Reliability Engineering & System Safety, 2016, 155: 97–104
16. Wang L, Shen T, Chen C, et al. Dynamic reliability analysis of gear transmission system of wind turbine in consideration of randomness of loadings and parameters. Mathematical Problems in Engineering, 2014, 2014: 261767
17. Tan X F, Xie L Y. Fatigue reliability evaluation method of a gear transmission system under variable amplitude loading. IEEE Transactions on Reliability, 2019, 68(2): 599–608
18. Yan Y Y. Load characteristic analysis and fatigue reliability prediction of wind turbine gear transmission system. International Journal of Fatigue, 2020, 130: 105259
19. Han W, Zhang X L, Huang X S, et al. A time-dependent reliability estimation method based on Gaussian process regression. In: Proceedings of the ASME International Design Engineering Technical Conferences and Computers and Information in Engineering Conference. Quebec City: ASME, 2018, V02AT03A056
20. Wei F, Lin H. Multi-objective optimization of process parameters for the helical gear precision forging by using Taguchi method. Journal of Mechanical Science and Technology, 2011, 25(6): 1519–1527
21. Korta J A, Mundo D. Multi-objective micro-geometry optimization of gear tooth supported by response surface methodology. Mechanism and Machine Theory, 2017, 109: 278–295
22. Savsani V, Rao R V, Vakharia D P. Optimal weight design of a gear train using particle swarm optimization and simulated annealing algorithms. Mechanism and Machine Theory, 2010, 45(3): 531–541
23. Zhu C C, Xu X Y, Lu B, et al. Fuzzy reliability optimization for transmission system of high-power marine gearbox. Journal of Ship Mechanics, 2010, 14(8): 915–921 (in Chinese)
24. Qin D T, Xing Z, Wang J. Optimization design of system parameters of the gear transmission of wind turbine based on dynamics and reliability. Chinese Journal of Mechanical Engineering, 2008, 44(7): 24–31
25. Zhang G Y, Wang G Q, Li X F, et al. Global optimization of reliability design for large ball mill gear transmission based on the Kriging model and genetic algorithm. Mechanism and Machine Theory, 2013, 69: 321–336
26. Wang Q Q, Wang H. Reliability optimization design of the gear modification coefficient based on the meshing stiffness. In: Proceedings of the 2nd International Conference on Advances in Materials, Machinery, Electronics. Xi'an: AMME, 2018, 1955: 030015
27. Tong C, Tian Z. Optimization design of gear reducer based on multi-attribute decision making and reliability sensitivity. In: Proceedings of the International Conference on Optoelectronic Science and Materials. Hefei: IOP, 2020, 711: 012045
28. Spinato F, Tavner P J, van Bussel G J W, et al. Reliability of wind turbine subassemblies. IET Renewable Power Generation, 2009, 3(4): 387–401
29. Li Y, Zhu C C, Tao Y C, et al. Research status and development tendency of wind turbine reliability. China Mechanical Engineering, 2017, 28(9): 1125–1133 (in Chinese)
30. Wang W, Liu H J, Zhu C C, et al. Effect of the residual stress on contact fatigue of a wind turbine carburized gear with multiaxial fatigue criteria. International Journal of Mechanical Sciences, 2018, 151: 263–273
31. Qin D T, Zhou Z G, Yang J, et al. Time-dependent reliability analysis of gear transmission system of wind turbine under stochastic wind load. Chinese Journal of Mechanical Engineering, 2012, 48(3): 1–8
32. International Electrotechnical Commission. IEC 61400-4:2012. Wind Turbines—Part 4: Design Requirements for Wind Turbine Gearboxes. 2012
33. Sun W, Li X, Wei J. An approximate solution method of dynamic reliability for wind turbine gear transmission with parameters of uncertain distribution type. International Journal of Precision Engineering and Manufacturing, 2018, 19(6): 849–857
34. Gao J X, An Z. A new probability model of residual strength of material based on interference theory. International Journal of Fatigue, 2019, 118: 202–208
35. Lin X, Wei J, Lai Y, et al. Gear residual strength model and dynamic reliability. Journal of Harbin Engineering University, 2017, 38(9): 1476–1483 (in Chinese)
36. He H F, Liu H J, Zhu C C, et al. Study of rolling contact fatigue behavior of a wind turbine gear based on damage-coupled elastic-plastic model. International Journal of Mechanical Sciences, 2018, 141: 512–519
37. Schaff J R, Davidson B D. Life prediction methodology for composite structures. Part I—Constant amplitude and two-stress level fatigue. Journal of Composite Materials, 1997, 31(2): 128–157
38. International Organization for Standardization. ISO 6336-2-2019. Calculation of Load Capacity of Spur and Helical Gears—Part 2: Calculation of Surface Durability (pitting). 2019
39. International Organization for Standardization. ISO 6336-3-2019. Calculation of Load Capacity of Spur and Helical Gears—Part 3: Calculation of Tooth Bending Strength. 2019
40. Evans M H. White structure flaking (WSF) in wind turbine gearbox bearings: Effect of 'butterflies' and white etching cracks (WECs). Materials Science and Technology, 2012, 28(1): 3–22
41. Li M, Xie L, Ding L. Load sharing analysis and reliability prediction for planetary gear train of helicopter. Mechanism and Machine Theory, 2017, 115: 97–113
42. Wei J, Pan Z, Lin X Y, et al. Copula-function-based analysis model and dynamic reliability of a gear transmission system considering failure correlations. Fatigue & Fracture of Engineering Materials & Structures, 2019, 42(1): 114–128
43. International Organization for Standardization. ISO 6336-5:

Calculation of Load Capacity of Spur and Helical Gears—Part 5: Strength and Quality of Materials. 2017

44. Aghili S J, Hajian-Hoseinabadi H. The reliability investigation considering data uncertainty; an application of fuzzy transformation method in substation protection. International Journal of Electrical Power & Energy Systems, 2014, 63: 988–999